J2.11

ANALYSIS OF THREE YEARS OF BOUNDARY LAYER OBSERVATIONS OVER THE GULF OF MEXICO AND ITS SHORES

Steven R. Hanna*
Hanna Consultants, Kennebunkport, Maine

Clinton P. MacDonald, Mark A. R. Lilly, and Charley A. Knoderer
Sonoma Technology, Inc., Petaluma, California

C.H. Huang
Minerals Management Service, New Orleans, LA

1. INTRODUCTION

There is a need to calculate the transport and dispersion of pollutants emitted from offshore oil and gas exploration and production activities in the Gulf or Mexico. However, much uncertainty exists concerning the atmospheric boundary layer in the region, due to space and time variations caused by variable underlying water temperatures and the effects of mesoscale atmospheric phenomena. The current study, supported by the Minerals Management Service, has involved instrumentation of six oil platforms to obtain boundary layer observations, including 915-MHz radar wind profilers (RWPs), 2-KHz Radio Acoustic Sounding Systems (RASS), and near-surface routine meteorology instruments. Two of these profiler sites have operated from May 1998 through September 2001 and four operated from October 2000 through September 2001. The profilers measure winds and RASS measures virtual temperatures between heights of about 100 m and a few kilometers. The near-surface observations at the oil platforms include sea surface temperature as well as wind speed, wind direction, air temperature, and mixing ratio at a reference elevation, z_r, of about 25 m (i.e., the platform elevation). These new data, in addition to the traditional data collected by buoys and available from the National Climatic data Center (NCDC), have been analyzed to investigate the overwater surface energy balance and boundary layer structure for both steady-state horizontally homogeneous conditions and for conditions variable in time and space. These three-dimensional, time-dependent fields are being used for analysis of transport and dispersion from overwater sources. Figure 1 shows a map of the Gulf of Mexico region and indicates the locations of the various observing sites.

The TOGA-COARE marine boundary layer algorithms (Fairall et al., 1996) have been used to analyze hourly-averaged and monthly-averaged fundamental boundary layer scaling parameters such as the surface roughness length (z_o), the friction velocity (u*), the scaling temperature (T*), the scaling water vapor mixing ratio (q*), and the Monin-Obukhov length (L), in addition to the latent and sensible heat fluxes. From these parameters, the mixing depth (h), and the vertical profiles of wind speed, temperature, and water vapor mixing ratio have been estimated. The basic structure of the COARE marine boundary-layer model is an outgrowth of the Liu-Katsaros-Businger (LKB) (Liu et al., 1979) method. Version 2.6bw of COARE , used in the current analysis, incorporates wave height and period data, in order to increase the accuracy of the estimates of surface fluxes and scaling parameters over shallow areas (Taylor and Yelland, 2000). The characteristics of waves differ from the deep ocean to the shallow coastal waters.

In the sections below, the outputs of the COARE program (e.g., boundary layer scaling parameters and energy fluxes) and the estimated profiles have been compared to observations and to simulations by the Eta numerical weather prediction model. In addition, some comparisons are presented of the observed RWP winds and the Eta/EDAS modeled winds (Black, 1994 and Rogers et al., 1997).

This paper describes a few highlights from the comprehensive observation and analysis project reported by MacDonald et al. (2004). Readers should note that this study focuses on the Western and Central Gulf of Mexico, west of the Florida – Alabama border. Additional studies, supported by the MMS, by other government agencies, and by industrial associations, are focusing on the eastern Gulf of Mexico region.

2. APPLICATION OF THE COARE MODEL

The COARE model requires the following input data: time and site location; wind speed, air temperature, and relative humidity (RH) within the surface layer at reference height z_r; sea surface skin temperature (T_s) or sea temperature near the surface plus radiation estimates; and mixing height. If the near-surface sea temperature is used, then solar and downwelling longwave radiation fluxes need to be estimated from some alternate source in order to correct this temperature to a skin temperature. Precipitation data is not required, but if available, can be used by COARE to

---

Corresponding author address: Steven R. Hanna, 7 Crescent Ave., Kennebunkport, ME 04046; e-mail: hannaconsult@adelphia.net

estimate the precipitation contribution to the energy balance equation. Wave height and period data are not required, but, when available, have been used with Version 2.6bw to account for the different wave structures and theoretically improve the accuracy of the estimates of surface fluxes and scaling parameters over shallow ocean areas. Data were acquired and processed from the following sites: 1998 through 2001 offshore buoy data from seven sites, shoreline CMAN station data from five sites, and data collected as part of this project on the Vermillion (VRM), South Marsh Island (SMI), Breton Island (BI), Fort Morgan (FM), Deep Water Platform (DWP), and Shallow Water Platform (SWP) oil platforms. Figure 1 shows the locations of the offshore buoys, the CMAN stations, and the oil platforms (with surface observations plus profilers).

The CMAN stations are located in very shallow water on the coast. Since the COARE model is not currently designed to use data collected in such areas, the data from these sites were used only in test exercises to evaluate how COARE would respond compared to open water sites. The data collected at the platforms meet the COARE input data requirements. The data collected at buoys meet most of the COARE data requirements, with the exception that solar and longwave radiation were not observed. Instead, radiation fluxes were estimated using 6-hourly ETA model cloud simulations and sun elevation data to calculate the water skin temperatures from water temperatures at depths of about 0.5 to 1.0 m.

The climatological part of the study is discussed first. Using the hourly meteorological data collected for over three years, hourly sensible heat flux, latent heat flux, surface stress, frictional velocity, temperature and relative humidity scaling parameters, z_r/L, and roughness length were calculated using COARE for 11 sites where the data passed QA procedures. Monthly statistics were then calculated from these hourly values. Monthly averages were not computed if more than 80% of the data in a given month were missing.

The case study part of the analysis is discussed second. In this analysis, time series of hourly-averages of selected meteorological and derived boundary layer parameters were created using COARE, for several five-day periods during different seasons. The analysis included comparisons of derived outputs from COARE with simulations of the Eta model for sensible and latent heat flux, and friction velocity.

3. RESULTS OF CLIMATOLOGICAL STUDY WITH COARE

The key results of the climatological study (comparisons of monthly averages) with COARE are briefly summarized in this section. The project report (MacDonald et al., 2004) discusses these points in detail and contains almost 200 figures illustrating the results.

The fluxes and scalar parameters calculated by the COARE algorithm in the Gulf of Mexico are physically consistent with our intuitive expectations, and are similar to observations and COARE calculations for TOGA, which took place in the warm Western Pacific Ocean near the equator (Fairall et al., 1996). Calculated sensible heat fluxes in the Gulf of Mexico average about 5 to 30 W/m^2, typical of other over-water sites. Similarly, calculated latent heat fluxes average about 50 to 100 W/m^2, also typical of other over-water sites. Calculated monthly-average sensible heat fluxes are about 1/5 of the calculated monthly-average latent heat fluxes and are generally greatest in the winter and early spring at all sites with the exception of GDIL1, which had no distinct yearly cycle. The approximate 1/5 ratio is found at other open-water sites at this latitude.

The fluxes tend to be strongly related to the sea-air temperature difference. Figure 2 contains monthly-averaged observed sea-air temperature difference over the three year period at seven buoys, two CMAN sites, and the VRM and SMI oil platforms (see Figure 1 for the locations). An annual variation is seen with maximum differences (about 2 to 4 C) in winter. Our analysis shows that the sea-air temperature difference is positive over 90 % of the time, implying that well-mixed conditions occur most of the time.

The COARE-calculated monthly-average sensible heat fluxes over the three year period at the same 11 sites used in Figure 2 are given in Figure 3. Slightly higher sensible heat fluxes (about 20 to 70 W/m^2) are calculated in the winter months, due to larger sea-air temperature differences and stronger winds during the winter. The sensible heat fluxes at the 11 sites tend to agree within a factor of two most of the time. Larger differences between sites are found in the summer months, when sensible heat fluxes are relatively small (about 10 W/m^2 or less) and are sometimes very near zero or are negative.

The COARE-calculated monthly average latent heat fluxes are shown in Figure 4 for the same 11 sites used in Figure 3. As mentioned above, the latent heat fluxes are about a factor of five larger than the sensible heat fluxes. The magnitudes of the fluxes are generally greater in the fall months, likely due to the higher water temperatures at that time. As is well-known, the annual maximum and minimum water temperatures have a time lag of a few months after the maximum and minimum air temperatures. Latent heat fluxes over the Gulf of Mexico are hardly ever negative due to the fact that the air at the surface is obviously always saturated with water vapor and the sea-air temperature difference is positive 90 % of the time. The latent heat fluxes in Figure 4 range from about 30 to 250 W/m^2. The shallow-water site of GDIL1 and the near-shore platform, VRM, generally have the greatest latent heat fluxes and highest water temperatures of all the sites during the spring and summer months.

Several plots of the COARE-calculated monthly average friction velocity, u*, temperature scaling parameter, T*, and humidity scaling parameter, q*, are given by MacDonald et al. (2004) but are not given in the current paper due to space limitations. The plots of u* would show an agreement among the sites well within a factor of two and often within 20%. This agreement is important because u* is the key scaling velocity for estimating transport speeds and dispersion rates. u* is calculated to be slightly lower from May through August when wind speeds are lower. The T* and q* plots also generally show a factor of two or better agreement among sites. T* and q* tend to be smaller in April and May, when the difference between the surface water temperature and the air temperature is at its minimum, and tend to be larger in October and November, when the difference between the surface water temperature and the air temperature is at its maximum.

4. RESULTS OF CASE STUDIES WITH COARE

Time series of hourly averaged observations, COARE-model calculations, and Eta-model simulations of boundary layer parameters at the observing sites in the Gulf of Mexico have been analyzed for several multi-day case study periods in different seasons. A few of the results from two case studies are discussed here, and the report (MacDonald et al., 2004) contains several others, including about 75 figures.

Figure 5 presents a time series of the air and skin temperatures and wind speed for the 20-25 January time period from buoy 42040, which is located several 10s of km to the southeast of the Mississippi River delta (see Figure 1). There were exceptionally large swings in wind and air temperature during these five days, with air temperatures five to ten C cooler than the water temperatures for the first two days and for the last day and a half. Wind speeds were moderate to strong (about 5 to 15 m/s) during these periods. However, during the middle of the time period, the air warmed slowly to approach and even exceed the water temperature for over 12 hours. The winds dropped to nearly zero just before a frontal passage at about 3 am on 24 January, after which the air temperature dropped 5 C in an hour and wind speed rapidly increased to 16 m/s.

Figure 6 shows the COARE-calculated and Eta-simulated sensible heat fluxes during this time period. The COARE model is using the buoy-observed meteorological variables, and is seen to produce very large (for the ocean) fluxes with magnitudes of about 200 W/m^2 during the beginning and ending periods, when the water-air temperature differences were very large (5 to 10 C) and the wind speeds were also large (about 10 to 15 m/s). However, during the 12 to 15 hour period in the middle of the time series, when the air temperature exceeded the water temperature, the COARE-calculated sensible heat fluxes were negative (i.e., towards the water surface) with magnitudes of about 10 W/m^2. The Eta model simulations of sensible heat flux are only about 30 % larger than the COARE calculated values during the periods with large air-water temperature differences. However, during the middle period, the Eta model simulates very slightly positive (upward) sensible heat fluxes (about 0 to 20 W/m^2). We find this tendency for all sites and periods. That is, occasionally the site shows periods with observed air temperatures warmer than water temperatures, leading to COARE-calculated negative heat fluxes, while the Eta model is simulated positive (but small) heat fluxes. During the late spring, when the air temperature is observed to be greater than the water temperature about 20 to 40 % of the time, this can lead to long periods of mismatches in the signs of the COARE and Eta simulated sensible heat fluxes.

Figure 7 presents a time series of the air and skin temperatures, wind speed, and relative humidity (RH) for a relatively warm period in September 18-20, 2001, for the South Marsh island (SMI) platform, which is located about 150 km south of the Louisiana coast. Temperatures were fairly constant at about 30 C and the sea-air temperature difference stayed at about 1 to 3 C during the period. Wind speed averaged about 3 m/s and dropped below 1 m/s during the afternoon of September 19 and the late evening of September 20. Figure 8 contains information on COARE estimated wave height and period and derived surface roughness length, z_o. The roughness length is about 0.00002 m most of the time, but increases, by a factor of about 25, to about 0.00055 m, during the light wind periods. This variation of roughness length is the opposite of what is expected, and is thought to be caused by possible errors in the revised roughness algorithm, which appears to be assuming that the waves in light winds generate a larger surface roughness.

Figure 9 shows the COARE-calculated and Eta-simulated sensible heat fluxes and latent heat fluxes during this time period. As expected, the latent heat fluxes are about 5 to 10 times larger than the sensible heat fluxes, when averaged over the three day period. The COARE and Eta estimates are seen to track each other fairly well (i.e., differences are less than a factor of two) most of the time. There are a few hours with large positive or negative differences between COARE and Eta, and these may be hours with cloud cover. We have not yet fully analyzed these differences.

Figure 10 contains the COARE and Eta-estimated friction velocities, u*, plus the COARE-estimated z/L.. The friction velocities are relatively small, averaging about 0.2 m/s, consistent with the light winds and small roughness length. About half of the time, the COARE u* estimates are less than the Eta estimates by about a factor of two. However, there is little bias the rest of the time, and there is better than factor of two agreement most of the time. z/L is typically about – 5, suggesting an unstable environment, as expected for light wind conditions with a positive sea-air temperature gradient and with humid conditions. Note that L includes the influence of both the sensible and latent heat fluxes.

5. COMPARISON OF WINDS FROM RADAR WIND PROFILER AND FROM ETA/EDAS PREDICTIONS

The six Radar Wind Profilers (RWPs) used during the study were shown in Figure 1. The RWPs were LAP-3000, 915-MHz boundary layer radars deployed on oil platforms. Two modes of data collection occurred at all RWP sites. The low mode represented 100-m resolution winds at heights from about 100 m above platform level (APL) to about 2000 m APL. The high mode represented 200-m resolution winds at heights from about 200 m APL up to about 4000 m APL. These RWP data were subjected to quality-control procedures by the authors. Typical problems that led to incorrect data were the presence of clutter due to sea waves and/or platform structures.

The EDAS model data represent bilinear interpolations of the 12-km Eta model output to a 40-km grid. Vertical interpolation is performed on the 12-km Eta model (60 levels) to the EDAS grid (39 levels). On the other hand, the RWP winds are a nearly-instantaneous volume-averaged measurement that is dependent on vertical resolution and beam width (approximately 3.5 km wide at 4 km above ground). The RWP data are averaged over one hour for comparison with the EDAS predictions.

Statistics were computed for those height bins containing at least 90% of the total number of RWP/EDAS possible data pairs. Sample sizes at each height and each RWP typically ranged from about 900 for the eastern sites associated with BAMP, to about 2000 for the western sites, which have been in operation for a longer period of time.

Figure 11 illustrates the wind speed and direction mean bias, mean standard deviation, and Mean Absolute Error (MAE) for the entire data collection period at all sites. In general, wind speeds were overestimated by the EDAS model by a slight amount, with more mean bias at the lower heights and with gradual improvement above 1000 m. The coastal land site, FTM, had the lowest wind speed mean bias, ranging from –1 to 0 m/s. VRM, BIP, and WDP all had wind speed mean biases generally between –2 (near the surface) and –1 m/s (aloft). The far offshore sites (SMI and DWP) had the highest wind speed mean biases of –3 (near the surface) to –2 m/s (aloft) and –6 (near the surface) to –1 m/s (aloft), respectively. These wind speed mean biases suggest that the EDAS model tends to overestimate wind speeds in offshore areas, with the difference increasing as distance from shore increases. The standard deviations of wind speed difference were 2 to 4 m/s and indicate little variation with altitude, which is somewhat surprising as lower standard deviations are expected aloft because the upper-level flow patterns are known to vary less than flows near the surface (Seaman, 2000).

Wind direction mean biases shown in Figure 11 were generally between –5° and 10° at all sites, with higher wind direction biases observed at heights below 1000 m at DWP (as high as 20°). DWP showed more wind direction mean bias near the surface, whereas the remaining sites tended to show a consistent mean bias with height. The mostly positive mean biases indicate that the EDAS model data had an overall counter-clockwise mean bias in wind direction. For example, with a 20° positive mean bias, if the observed mean wind direction were 180°, then the EDAS-predicted mean wind direction would be 160°. The standard deviations of wind direction differences were generally about 25° to 35° and showed little variation with height. While the wind direction mean biases at offshore sites were similar to those at the near-shore sites, the standard deviations of the wind direction differences were generally about 40° at the offshore sites. These standard deviation values for wind speed and wind directions (2 to 4 m/s and 20° to 50°) found for the six RWPs in the Gulf of Mexico domain agree well with standard deviations reported by Seaman (2000) and Hanna and Yang (2001) for other models and other geographic domains.

In general, the MAE between the EDAS-predicted and the RWP-observed wind speeds at all sites was largest near the surface and increased with increasing distance from the shoreline (see Figure 12). The coastal site, FTM, had a MAE of 1 to 2 m/s. VRM, BIP, and WDP had MAEs of about 2 m/s, excluding the lowest height. SMI was observed to have an MAE of 2 to 3 m/s, and DWP had an MAE of 2 to 6 m/s, with the largest MAEs near the surface in both cases. Because MAE is strongly influenced by the mean bias, the large 6 m/s MAE value at DWP near the surface is primarily due to the large mean bias of approximately the same magnitude.

The wind direction MAE is generally constant with height. The wind direction MAE was found to be between 15° and 25° at the coastal and near-shore sites and 25° to 35° at the offshore sites.

Comparisons between RWP-observed wind data and EDAS-modeled wind data over the Gulf of Mexico show better agreement at near-shore sites and poorer agreement at offshore sites. In general, the EDAS model tended to overstate wind speeds, especially at levels below 1500 m. The EDAS model tended to have a positive wind direction mean bias (i.e., if the observed wind direction were 180°, the predicted wind direction might be 160°); however, this mean bias was usually 10° or less. In considering these comparisons, it should be noted that the EDAS data is created by a bilinear interpolation of a fine-scale grid onto a more coarse grid resolution, whereas the RWP observations are a volume-averaged measurement in which the measurement representativeness can vary with fluctuations in the wind speed.

6. CONCLUSIONS AND RECOMMENDATIONS

The analysis used three years of observations of surface conditions and vertical profiles from several meteorological stations in the Gulf of Mexico. These new stations include 915-MHz radar wind profilers (RWP), 2-KHz Radio Acoustic Sounding Systems (RASS), and surface meteorological stations. Two stations collected data for three years from May 1998 through October 2001, and four stations collected data from September 2000 through October 2001. The RWPs and RASS measure winds and virtual temperatures (T_v), respectively, from near the surface to heights of a few kilometers, and the surface stations measure skin temperature as well as wind speed, wind direction, air temperature, and water vapor mixing ratio at an elevation of about 25 m on an oil platform. In addition to the new data from the vertical profilers, routine meteorological observations from buoys and from CMAN shoreline stations were included in the analysis.

The new data and the routine data have been combined in the analysis to investigate the over-water surface energy balance, and the climatology of latent heat fluxes, sensible heat fluxes, momentum fluxes, and moisture fluxes. Estimates of the scaling velocity (u*) and scaling temperature (T*) were studied. The widely-used COARE algorithm was used for estimation of surface fluxes based on routine measurements. Three-dimensional predicted fields of surface winds, heat and momentum fluxes, and wind profiles, from the National Center for Environmental Protection's (NCEP's) Eta model, were compared with the observations from the RFPs and buoys.

The differences between the observed water "skin" and air temperatures were, on average, +1 to +3°C at most sites all year. The differences were less in late spring and greater in late fall and early winter. The boundary layer was found to be unstable over 90 % of the time. Occasionally, very large stability or instability were observed near-shore with advection of warm air over cold water or cold air over warm water.

The fluxes and scaling parameters calculated by the COARE algorithm in the Gulf of Mexico are physically consistent with expectations and are similar in magnitude to the previous observations and COARE calculations for TOGA, which took place in the warm western Pacific Ocean near the equator. Calculated monthly average sensible heat fluxes in the Gulf of Mexico ranged from 5 to 30 W/m^2, typical of other over-water areas. Similarly, calculated monthly average latent heat fluxes ranged from 50 to 150 W/m^2, also typical of other over-water areas. Both the latent and sensible heat fluxes were highest in the late fall and early winter and lowest in the late spring and summer, although the yearly cycle in latent heat values is less pronounced. Sensible heat flux is maximized for post-trough synoptic conditions, which are likely to be marked by above average wind speeds and by low air temperature. The calculated fluxes are generally in good agreement with the monthly average Eta model latent and sensible heat fluxes.

The COARE-calculated monthly average friction velocity, u*, for the buoys, the C-MAN sites, and the SMI platform shows agreement among these sites well within a factor of two and often within 20%. This agreement is important because the monthly average friction velocity is the key scaling velocity for estimating transport speeds and dispersion rates. However the VRM, BIP, DWP, MBP, SWP, and WDP platforms (part of BAMP) suggest mean friction velocities that are 30% to 40% less than the other sites. Possible explanations are that the wave height and frequency are estimated from empirical relations given observations of wind speed at the platforms, whereas they are directly measured at the buoys. The monthly average Eta model friction velocity was usually within about 10 to 20 % of the COARE- calculated friction velocity.

The "open-ocean" COARE algorithm could not simulate the slight diurnal variations in fluxes observed at the C-MAN coastal stations, which have surface characteristics in-between those of water and land (some are in tidal marshes, some are on barrier islands, and some are on beaches).

The Eta/EDAS-simulated wind fields and the observed RWP winds from six sites were compared. EDAS is based on a combination of Eta model forecast winds and diagnostic interpolations of observed winds but does not include the RWP data. The mean wind speed (WS) bias was near zero close to the shore but increased with offshore distance, so that the EDAS mean wind speed exceeded the RWP mean wind speed by 1 to 2 m/s at 50 km offshore and by 2 to 6 m/s at 100 to 200 km offshore. Mean wind direction (WD) bias was small, about a 10° to 20° difference (e.g., if the RWP WD was 180°, then the EDAS WD would be 160°). Standard deviations of the differences (with mean bias removed) were 1 to 2 m/s for WS and 20° to 40° for WD, in agreement with findings for other domains and models. However, these comparisons primarily focus on heights of a few hundred meters, since, due to sea clutter, the RWP seldom provided observations at heights less than about 200 m.

The following recommendations are made for future studies:

- Develop a better understanding of the reasons for the over-water wind differences between the Eta model and observed RWP winds. Analysis has shown that Eta model winds are biased high compared to RWP winds away from shore.
- Improve COARE algorithms for shallow water conditions with light wind speeds, where surface roughness is overpredicted. This bias influences estimations of other boundary layer parameters.
- Because accurate spatial sea-surface temperatures are important for accurate modeling, compare

satellite-derived sea-surface temperatures to radiometer temperatures and buoy temperatures measured during this study. Compare estimates of sea-surface temperatures to the radiometer temperatures when clouds obscure the satellite's view of the Gulf (currently estimated using hole-filling techniques).

- Identify several additional periods of super-stable conditions in the existing data set (i.e., a period of southerly flow occurring immediately after a cold outbreak has cooled the water in the shallow portion of the Gulf) and perform an ABL case study similar to other case studies.
- When wave data is not available at the platforms, inaccurate knowledge of wave characteristics can result in inaccurate estimates of surface roughness, which influence ABL parameterizations. Determine the best method for estimating wave height and frequency as a function of water depth from wind speed alone.
- Collocate a radiometer and underwater temperature sensor to better determine the relationship and accuracy of the COARE-estimated warm-layer and cool-skin effect.
- Routinely operate a measurement system on an offshore platform that measures a range of meteorological parameters at several depths of the surface layer and boundary layer. Such a system could include a mini-Sodar, an RWP/RASS system, and a surface meteorological monitoring system on a platform to obtain wind and temperature measurements. The addition of the mini-Sodar would fill the measurement void that exists from 30 m to 200 m; this hole is often the location of plumes.
- To better characterize the ABL over the shoreline of the western and central Gulf of Mexico, an enhanced field experiment should be planned, including shoreline surface towers with flux observations, minisodars (to provide data below 200 m) at the RWP stations, and a focused study with several surface stations and profilers along a cross-section from 10 km offshore to 10 km onshore at a marshy location.

ACKNOWLEDGEMENTS

This research was sponsored by the Minerals Management Service of the U.S. Department of Interior. The authors appreciate the technical advice from Dr. Christopher Fairall, the developer of the COARE model, and the assistance given by numerous persons responsible for meteorological data collection on the oil platforms.

REFERENCES

Black, T., 1994: The new NMC mesoscale Eta model: description and forecast examples. *Wea. Forecasting*. **9**, 265-278.

Fairall, C.W., E.F. Bradley, D.P. Rogers, J.B. Edson, G.S. Young, 1996: Bulk parameterization of air-sea fluxes for TOGA COARE. J. Geophys. Res. 101, 3747-3764.

Hanna, S.R. and R. Yang, 2001: Evaluations of mesoscale model predictions of near-surface winds, temperature gradients, and mixing depths. J. Appl. Meteorol., 42, 453-466.

Liu, W.T, K.B. Katsaros and J.A. Businger, 1979: Bulk parameterization of the air-sea exchange of heat and water vapor including the molecular constraints at the interface, J. Atmos. Sci. 36, 1722-1735.

Macdonald, C.P. et al., 2004: Boundary Layer Study in the Western and Central Gulf of Mexico. Final report STI-998555-2266-FR, STI, 1360 Redwood Way, Suite C, Petaluma, CA 94954-1169, prepared for Minerals Management Service, New Orleans, LA

Rogers E., Baldwin M., Black T., Brill K., Chen F., DiMego G., Gerrity J., Manikin G., Mesinger F., Mitchell K., Parrish D., and Zhao Q., 1997: Changes to the NCEP operational "Early" Eta Analysis/Forecast System. Technical Procedures Bulletin, Series No. 447, National Weather Service, Office of Meteorology, December. Available on the Internet at http://www.nws.noaa.gov/om/tpb/447.htm

Seaman, N.L., 2000: Meteorological modeling for air quality assessments. Atmos. Environ. 34, 2231-2259.

Taylor, P.K., and M.J. Yelland, 2000: The dependence of sea surface roughness on the height and steepness of the waves. *J. Phys. Oceanography*, **31**, 572-590.

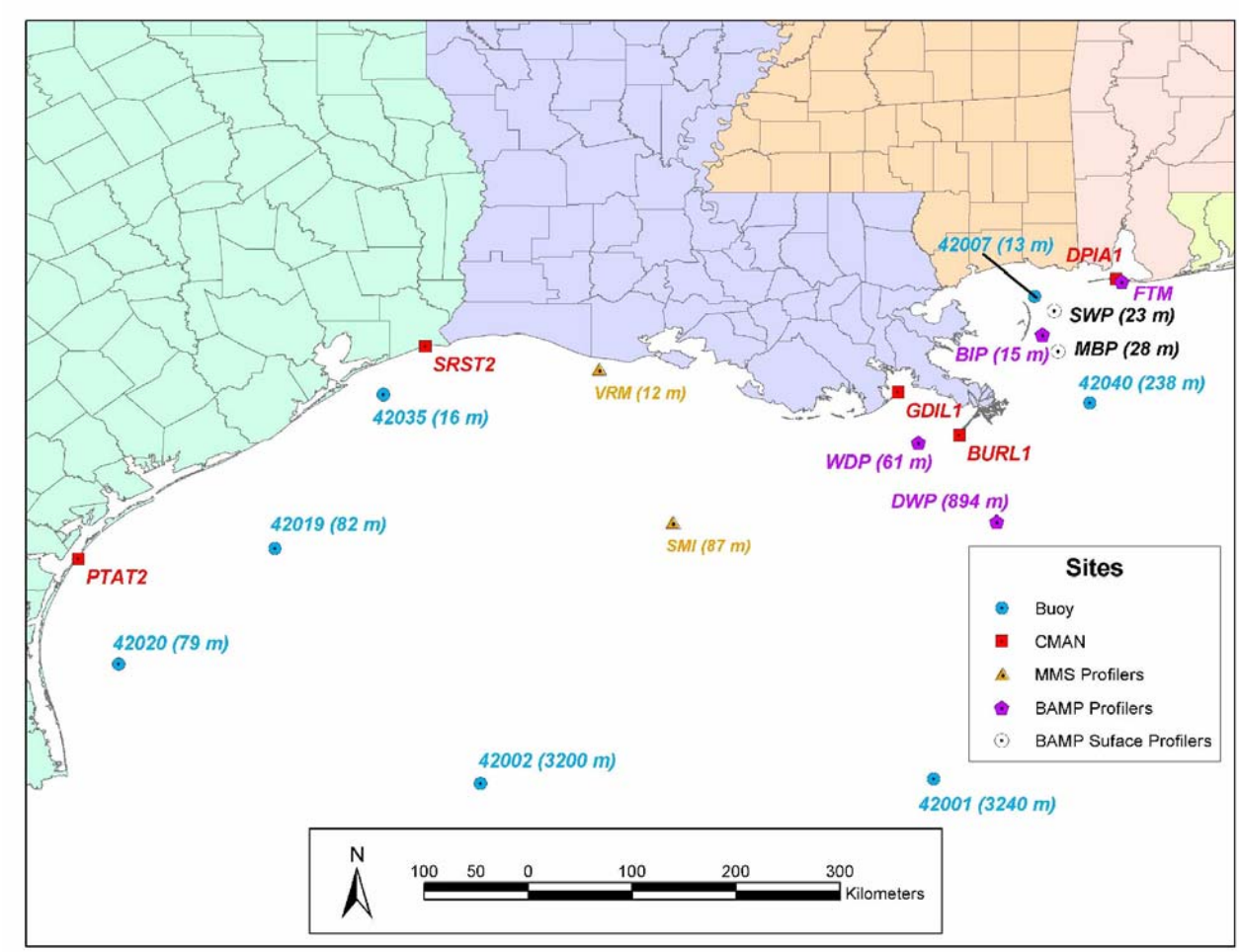

Figure 1. Map of the MMS study region depicting locations of CMAN, buoy, and platform profilers.

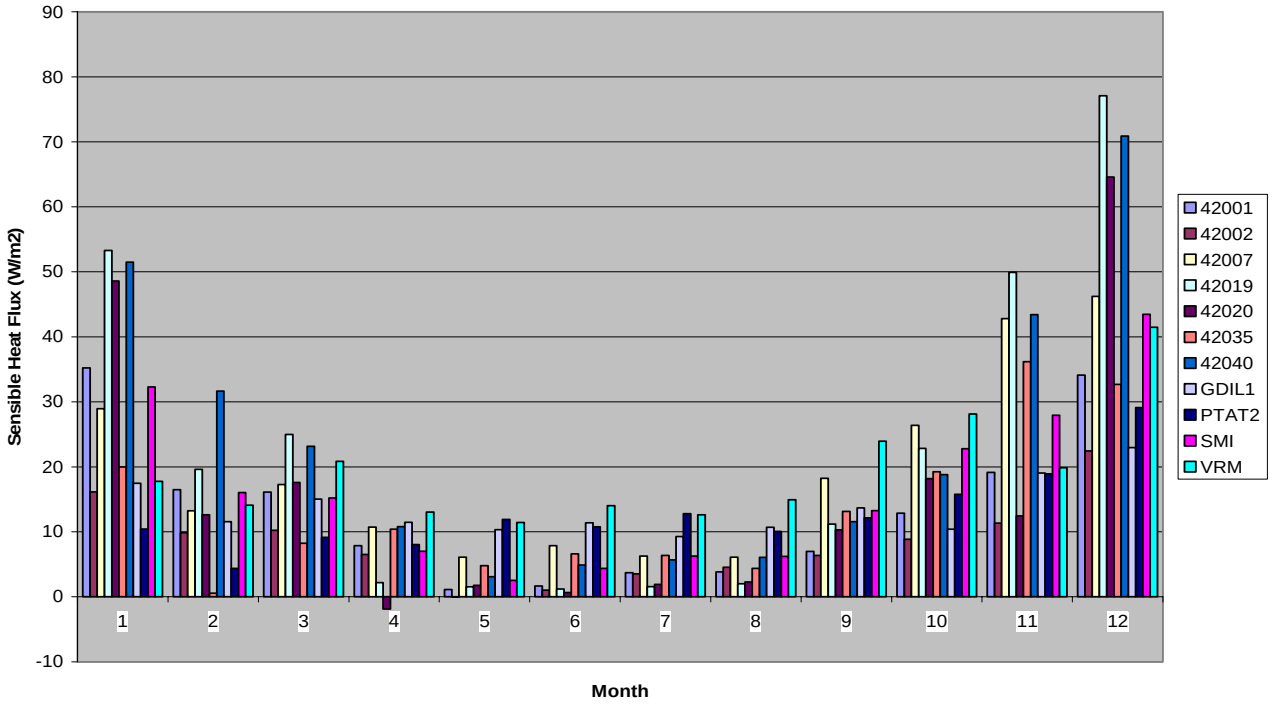

Figure 2. Monthly averages of COARE-estimated sensible heat fluxes by site for May 1998 through October 2001.

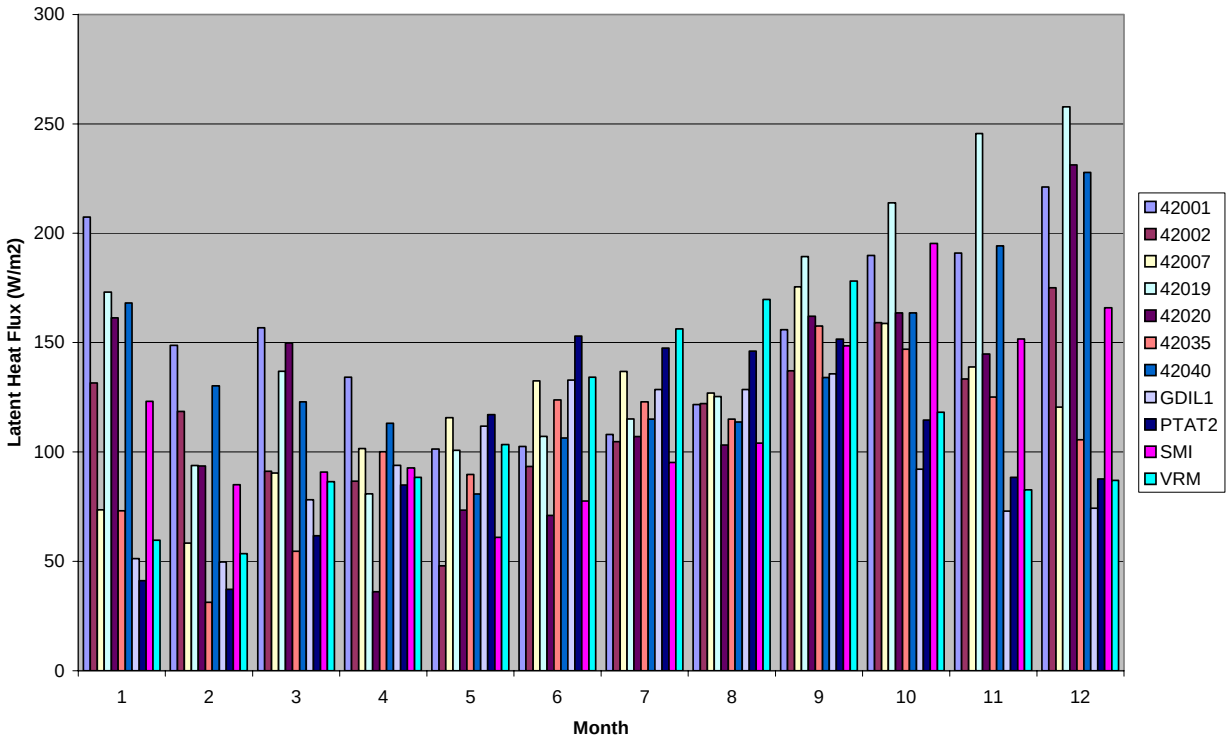

Figure 3. Monthly averages of COARE-estimated latent heat fluxes by site for May 1998 through October 2001.

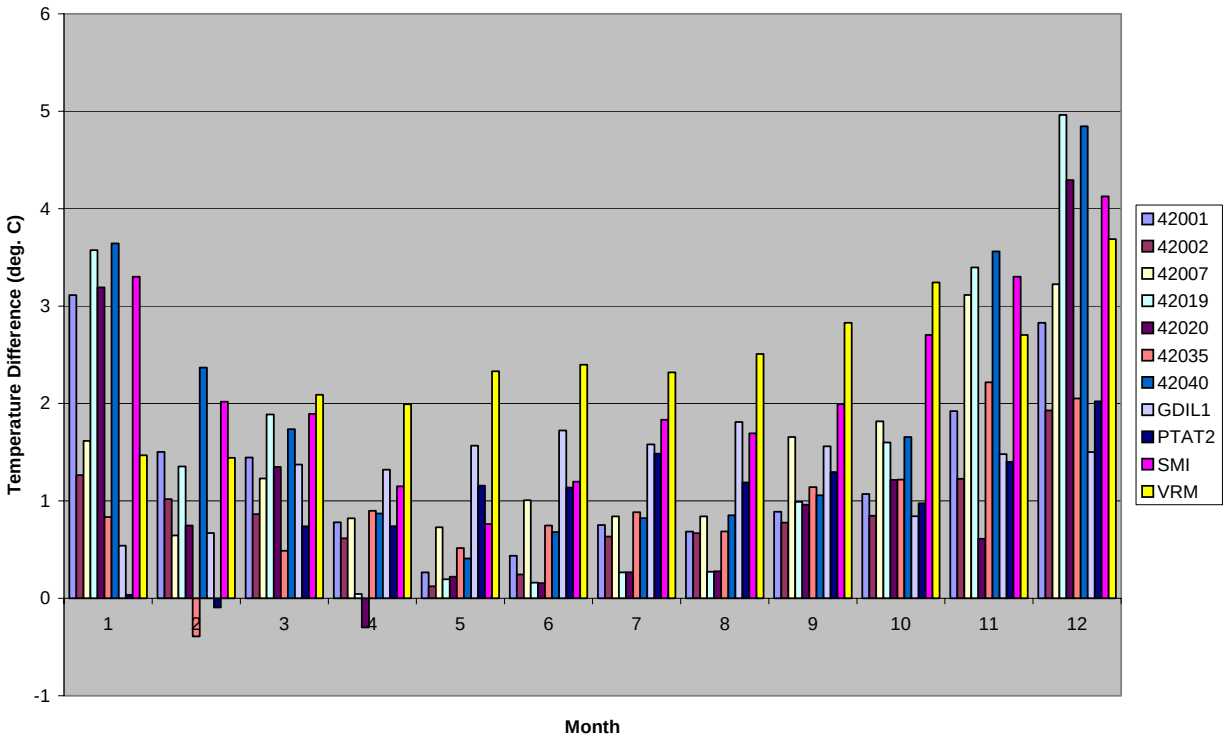

Figure 4. Monthly averaged observed skin (water surface) temperature minus air temperature by site for May 1998 through October 2001. The skin temperature was observed only at the platforms (SMI and VRM) and was estimated by COARE from the observed water temperature (at a depth just below the surface) at the other sites.

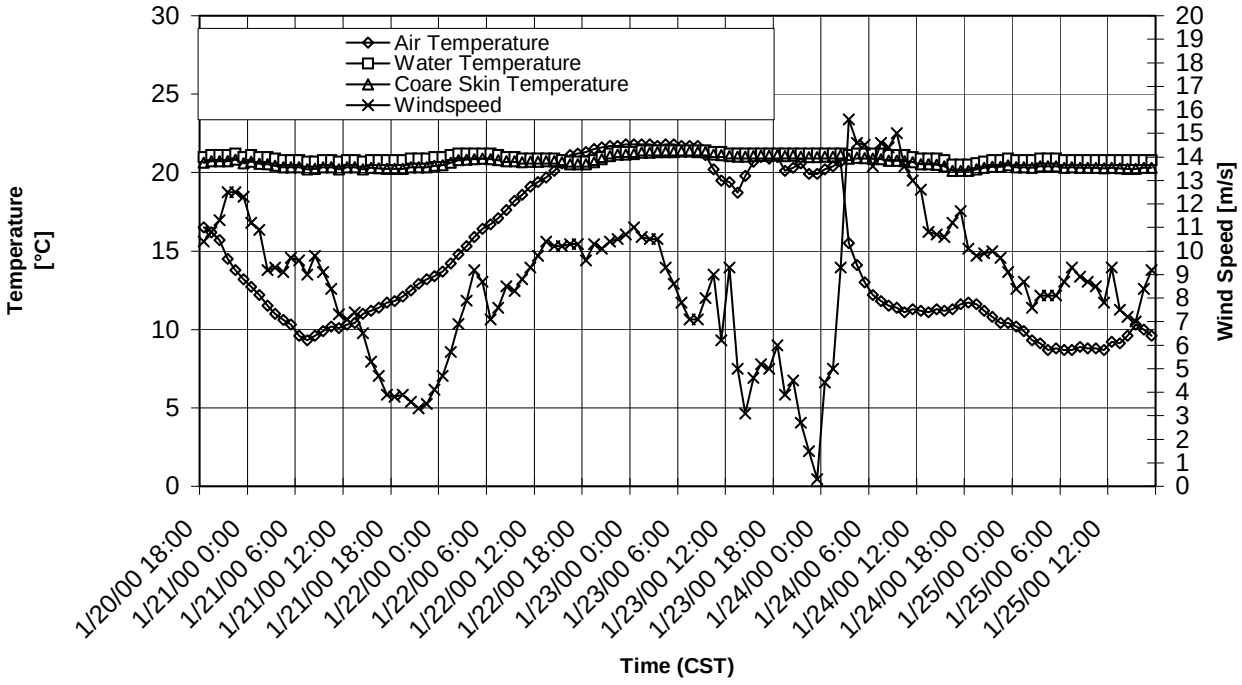

Figure 5. Observed air and water temperatures and COARE-estimated skin (water surface) temperature, and observed wind speed at buoy 42040 for January 20 through 25, 2000.

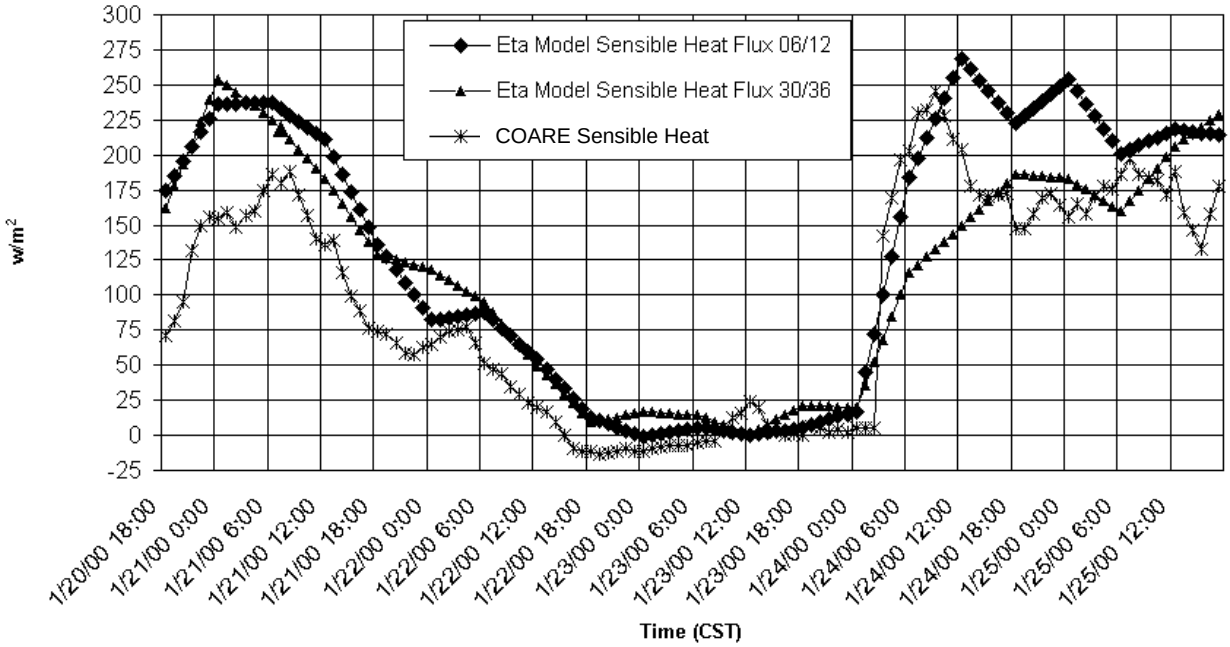

Figure 6. Estimated COARE and simulated Eta hourly sensible heat fluxes at buoy 42040 for January 20 through 25, 2000. Eta-simulated sensible heat fluxes were obtained from the 6- and 12-hr and the 30- and 36-hr forecasts and interpolated to hourly values between the 6- and 12-hr and the 30- and 36-hr forecasts.

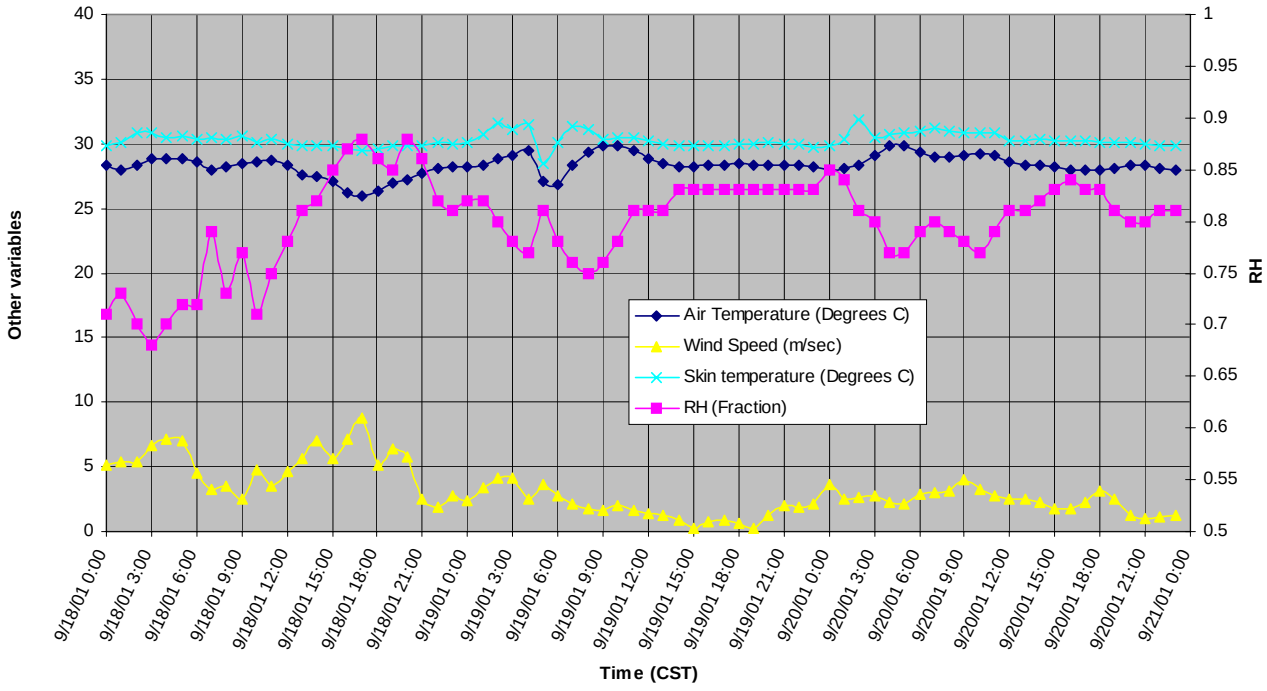

Figure 7. Observations of hourly air and skin (water surface) temperatures, wind speed, and relative humidity (RH) at SMI for September 18 through 20, 2001.

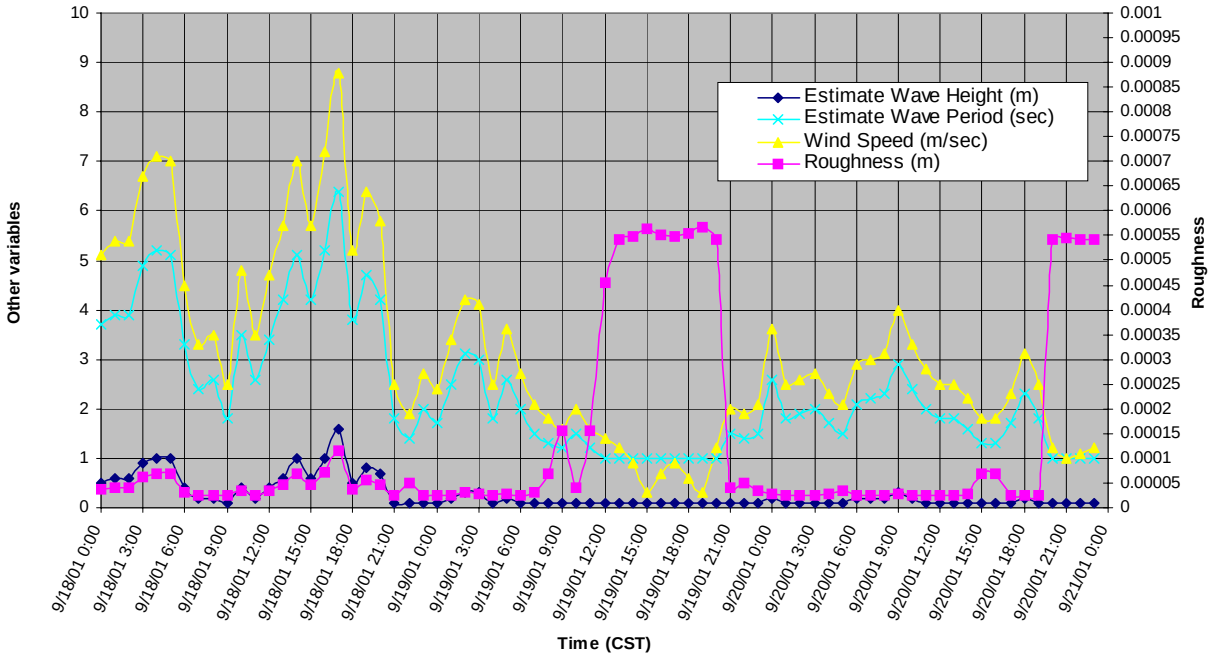

Figure 8. Estimated wave height and period, observed wind speed, and estimated surface roughness length at SMI for September 18 through 20, 2001.

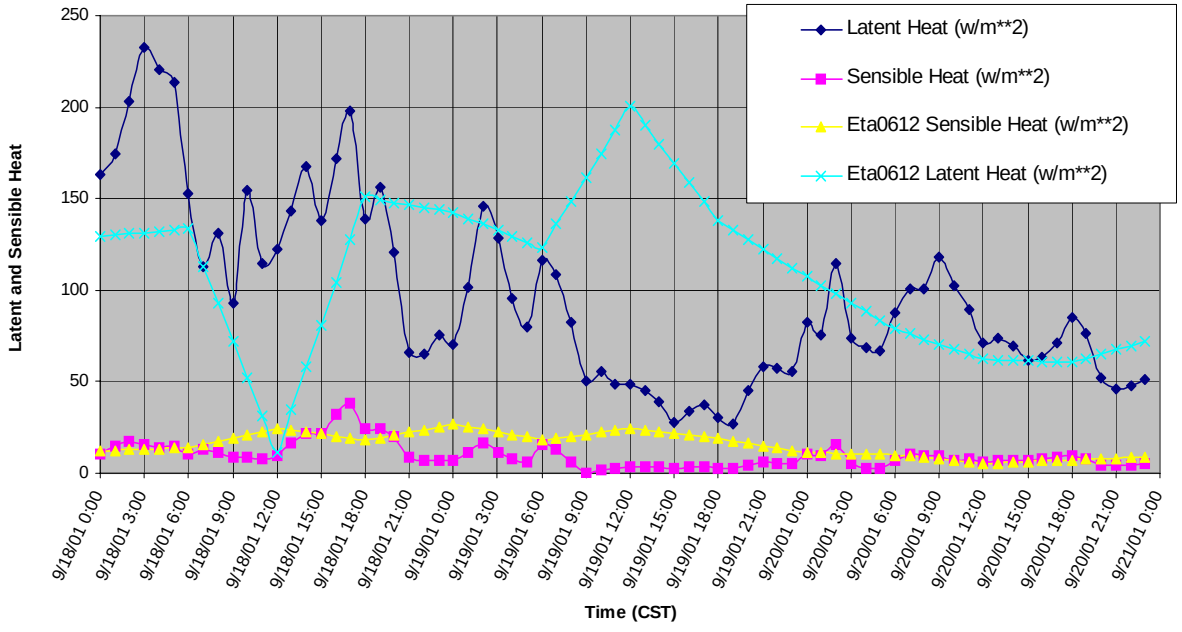

Figure 9. COARE and Eta latent and sensible heat fluxes at SMI for September 18 through 20, 2001. Note: the four-digit number after Eta in the key indicates the forecast period (i.e., 0612 is the 6- to 12-hr forecast).

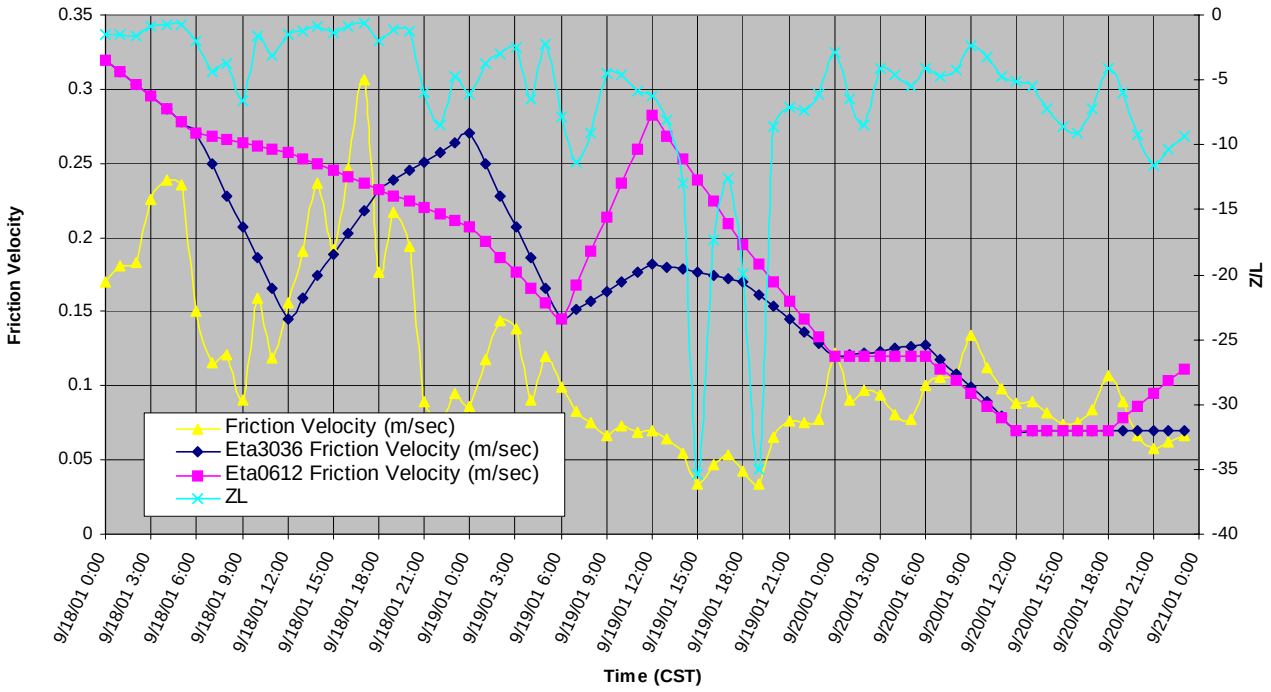

Figure 10. COARE and Eta friction velocity and z/L at SMI for September 18 through 20, 2001. Note: the four-digit number after Eta in the key indicates the forecast period (i.e., 0612 is the 6- to 12-hr forecast and 3036 is the 30- to 36-hr forecast).

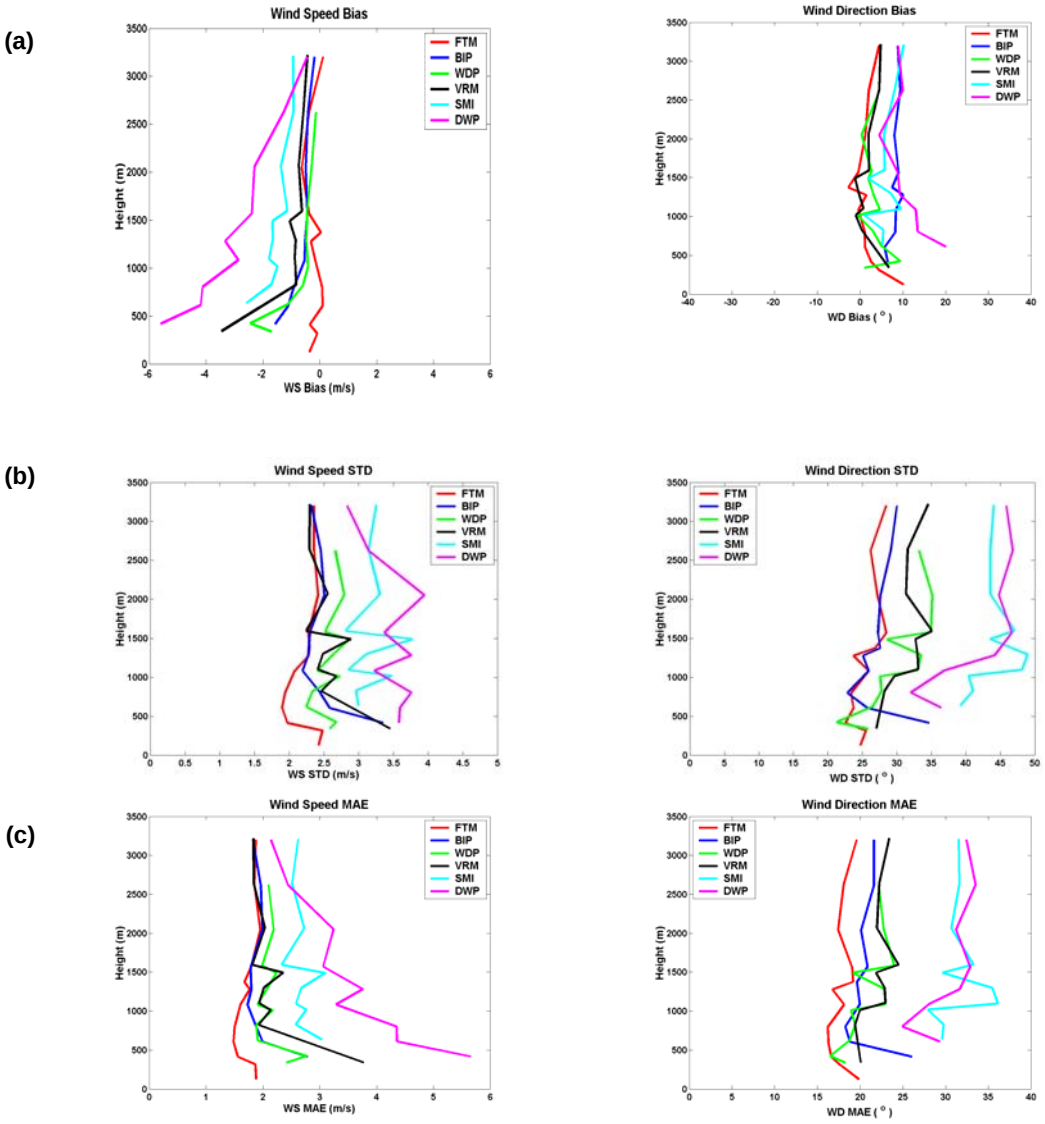

Figure 11. Comparison of Radar Wind Profiler (RWP) observed wind speeds and directions with EDAS simulations: (a) wind speed and direction mean bias, (b) mean standard deviation (STD), and (c) mean absolute error (MAE) for the six RWP sites shown in Figure 1.